Environmental Pollution 220 (2017) 843–852

Contents lists available at ScienceDirect

Environmental Pollution

journal homepage: www.elsevier.com/locate/envpol

Endosulfan induces autophagy and endothelial dysfunction via the AMPK/mTOR signaling pathway triggered by oxidative stress☆

Lianshuang Zhang [a, b, c], Jialiu Wei [a, b], Lihua Ren [a, b], Jin Zhang [a, b], Ji Wang [a, b], Li Jing [a, b], Man Yang [a, b], Yang Yu [a, b], Zhiwei Sun [a, b], Xianqing Zhou [a, b, *]

[a] Department of Toxicology and Hygienic Chemistry, School of Public Health, Capital Medical University, Beijing 100069, China
[b] Beijing Key Laboratory of Environmental Toxicology, Capital Medical University, Beijing 100069, China
[c] Department of Histology and Embryology, Bin Zhou Medical College, Yan Tai 264003, China

ARTICLE INFO

Article history:
Received 16 August 2016
Received in revised form
19 October 2016
Accepted 23 October 2016
Available online 1 November 2016

ABSTRACT

Cardiovascular diseases is related to environmental pollution. Endosulfan is an organochlorine pesticide and its toxicity has been reported. However, the relationship between oxidative stress and autophagy induced by endosulfan and its underlying mechanism remain confusing. In this study, human umbilical vein endothelial cells (HUVECs) were chosen to explore the toxicity mechanism and were treated with 0, 1, 6, 12 $\mu g/mL^{-1}$ endosulfan for 24 h, respectively. The present results showed that autophagy could be induced by endosulfan, which was verified by the monodansylcadaverine staining, autophagic ultrastructural observation, and LC3-I/LC3-II conversion. In addition, the levels of adenosine triphosphate (ATP), the mitochondria membrane potential (MMP) were significantly decreased in a dose-dependent way. The expression of proinflammatory cytokines (tumor necrosis factor α, interleukin-1β, and interleukin-6) were significantly elevated, and the index of endothelial function such as monocyte chemotactic protein 1 (MCP-1), intercellular cell adhesion molecule-1 (ICAM-1) increased. Moreover, endosulfan had an activation effect on the 5′AMP-activated protein kinase (AMPK)/rapamycin (mTOR) signaling pathway. Our findings demonstrated that endosulfan could induce oxidative stress and mitochondria injury, activate autophagy, induce inflammatory response, and eventually lead to endothelial dysfunction via the AMPK/mTOR pathway. This indicates that exposure to endosulfan is a potential risk factor for cardiovascular diseases.

1. Introduction

Endosulfan (6,7,8,9,10,10-hexachloro-1,5,5a, 6,9,9a-hexahydro-6,9-methano-2,4,3-benzodioxathiepine-3-oxide) is a cyclodiene broad organochlorine pesticide, which is.

widely used on wide variety of crops in many parts of the world (Mersie et al., 2003). As a result of its widespread use, it is an environmental contaminant and a public health hazard (Jaiswal et al., 2005). Endosulfan is hazardous to various organs including testes, kidney and immune (Ozmen and Mor, 2015; Choudhary and Joshi, 2003; Jamil et al., 2004; Aggarwal et al., 2008). However, there is still a lack of evaluation regarding the toxicity of endosulfan on cardiovascular system.

A growing body of literature suggests that apoptosis may contribute to the toxicity of POPs (Quan et al., 2014; Gregoraszczuk et al., 2008). But few study pay attention to the relationship between autophagy and POPs. Autophagy is defined as a protective mechanism in cells that can degrade proteins and/or damaged organelles to maintain cellular homeostasis (Teng et al., 2012). Nevertheless, the process of autophagy can be stimulated by oxidative stress (Liu et al., 2015; Li et al., 2015). Our previous study showed that endosulfan could activate extrinsic coagulation pathway by inducing endothelial cell injury via oxidative stress (Zhang et al., 2015). Whether endosulfan can induce autophagy and influence endothelial cell function is a crucial issue in human health and safety.

Endothelial dysfunction, first described by Panza et al. (Panza et al., 1990) Endemann and Schiffrin (Endemann and Schiffrin, 2004) is defined as a series of events, mainly including vasodilation reduction, proinflammatory response, and reducing of monocyte chemotactic protein 1 (MCP-1) and intercellular cell adhesion

☆ This paper has been recommended for acceptance by David Carpenter.

* Corresponding author. Department of Toxicology and Hygienic Chemistry, School of Public Health, Capital Medical University, Beijing 100069, China.
E-mail addresses: xqzhou@ccmu.edu.cn, xianqingzhou@aliyun.com (X. Zhou).

http://dx.doi.org/10.1016/j.envpol.2016.10.067
0269-7491/

molecule-1 (ICAM-1) (Catalán et al., 2015). Yet, the biological behavior and toxic effects of endosulfan on the vasculature is still poorly understood. In this study, we confirmed the association between endosulfan-induced autophagic activity and endothelial dysfunction by conducting a series of assessments in the human umbilical vein endothelial cells (HUVECs), such as oxidative stress, autophagy, release of cell adhesion cytokines and proinflammatory cytokine, we also examined the AMPK/rapamycin (mTOR) signaling pathway to explore the possible mechanism of the toxicity induced by endosulfan. These findings provide persuasive evidence for the toxic effects of endosulfan on the cardiovascular system.

2. Materials and methods

2.1. Cell culture and co-incubation with endosulfan

HUVECs were purchased from ATCC Manassas (No. CRL-1730), the cells were cultured in a humidified environment (37 °C; 5% CO2), maintained in Dulbecco's Modified Eagle's Medium (DMEM) (Hecolon; Thermo Fisher Scientific, Waltham, MA, USA) with 10% fetal bovine serum (Gibco; Thermo Fisher Scientific), 100 U/mL of penicillin and 100 μg/mL of streptomycin. For all tests, the HUVECs were seeded in six-well plates (1×10^5 cells/mL) and allowed to attach for 24 h; they were then exposed to different concentrations (1, 6 and 12 μg/mL) of endosulfan for another 24 h. *N*-acetyl cysteine (NAC) (Sigma, USA) was chosen as the antioxidant and Dorsomorphin (Dor) as the inhibitor of AMPK respectively. Considering the possible reaction between endosulfan and NAC or Dor, cells were pretreated with 3 mM/ml NAC and 20 μM/ml Dor for 2 h before exposure to endosulfan. The equivalent volume of culture medium without endosulfan was set as the control group. Five replicate wells were used in each treatment group.

2.2. Detection of mitochondria membrane potential (MMP)

MMP was detected by using the fluorescent probe JC-1 (Jiancheng, China). This probe can selectively enter into mitochondria and reversibly change color from red to green as the membrane potential decreased. The ratio of red to green expresses the change of MMP. Cells were treated with endosulfan for 24 h, after washing with PBS, the cells were incubated with 10 μg/mL working solution of JC-1 for 15 min at room temperature. Then the cells were collected and washed with PBS twice followed by flow cytometric (FCM) (Becton-Dickison, USA) analysis. The green fluorescence intensity was determined at an excitation wavelength of 488 nm and an emission wavelength of 525 nm, whereas the red fluorescence intensity was determined at an excitation wavelength of 488 nm and an emission wavelength of 590 nm. For each sample, at least 1×10^4 cells were collected.

2.3. ATP assay

The levels of ATP in the cells were measured using a firefly luciferase-based ATP assay kit (Jiancheng, nanjing, China), according to the manufacturer's instructions. After rinsing with phosphate-buffered saline (PBS), the cells were disrupted in 200 μl lysis buffer, and centrifuged at 12,000 rpm at 4 °C for 5 min, from which the supernatant was collected. In a 1.5 ml tube, a 100 μl sample of the supernatant was mixed with 100 μl ATP detection working solution. The luminance (RLU) was immediately measured using a Turner BioSystems luminometer (Promega Corporation, Madison, WI, USA). Standard curves for quantification were generated using known amounts of an ATP standard, and the protein concentration of each treatment group was determined using a bicinchoninic acid protein assay kit (Beyotime Institute of Biotechnology). Total ATP levels were expressed as μmol/g prot (Li et al., 2012).

2.4. Measurement of ROS and MDA

The ROS generation was measured through fluorescence intensity of dichlorofluorescein (DCF) by flow cytometry. After exposure to endosulfan for 24 h, cells were incubated in dark at 37°Cwith 2,7-dichlorofluorescein-diacetate (DCFH-DA, 100 ng/mL, Jiancheng, China) for 30min as previously described (Wang et al., 2009). Then the cells were washed twice with cold PBS and resuspended in PBS for further analysis. At last, the fluorescence intensity of 1×10^4 cells for each sample was measured by flow cytometry (Becton-Dickinson, USA).

The concentration of Malondialdehyde (MDA) as a marker of lipid peroxidation (LPO) was determined using an MDA kit. The assay mixture, including protein of cells, distilled water and sodium dodecyl sulfate (SDS) was incubated in a test tube at room temperature for 10 min, followed by the addition of a 20% acetic acid solution (1.0 ml, pH 3.5). After incubation for 10 min at 37 °C, 0.8% thiobarbituric acid (TBA) (1.0 ml) was added to the mixture. The reaction mixture was placed over a boiling water bath at 100 °C for 1 h. After n-butanol (4.0 ml) was added to the mixture, the organic layer was separated by centrifugation at 3000 rpm for 10 min at room temperature. The supernatant liquid was transferred to a fresh tube. The absorbance was measured at 532 nm with a microplate reader (DNM-9602G, China) using n-butanol as a standard. The data are shown as nmoles of MDA formed h-1 mg-1 protein.

2.5. Observation of mitochondria and autophagy by TEM

The cell samples were fixed overnight in 2.5% glutaraldehyde. Then, the samples were washed by 0.1 M PB for three times and postfixed with 1% osmic acid for 2 h. Then, a series of dehydration processes (50%, 70%, 80%, 90%, and 100% alcohol, and 100% acetone) was performed. After that, all the cell samples were embedded in epoxy resin. The thickness of the ultrathin sections was approximately 50 nm, which were made by an ultramicrotome (Ultracut UCT; Leica Microsystems). After being stained by lead citrate and uranyl acetate, these samples were observed under a TEM (JEM-2100; JEOL).

2.6. MDC staining

The fluorescent dye, monodansylcadaverine (MDC), is a special marker for autophagic vacuoles. HUVECs were stained with 0.1 mM of MDC (Jiancheng, China) for 15 min in the dark after the cells were exposed to endosulfan for 24 h. Then, the cells were washed with PBS three times. The visualization of MDC staining was detected by LSCM (Leica TCS SP5; Leica Microsystems). And the fluorescence intensity of 1×10^4 cells for each sample was measured by flow cytometry (Becton-Dickinson, USA).

2.7. Measurement of ICAM-1 and MCP-1

The supernatants were collected after the HUVECs were exposed to endosulfan for 24 h. The levels of MCP-1 and ICAM-1 were measured by enzyme-linked immunosorbent assay kits (Yuchen Biotechnology Company, Shanghai) according to the manufacturer's protocols. Briefly, 50 μl of supernatants were added in each well and incubated for 2 h at room temperature. Then, biotin antibody was added to each well and incubated for 1 h. After that, streptavidin solution was added and incubated for 30 min. Next, the substrate reagent was added and incubated for 30 min.

After the stop solution was added to each well, the absorbance at 450 nm was detected immediately using a microplate reader (Thermo Multiskan™ MK3; Thermo Fisher Scientific).

2.8. Measurement of proinflammatory cytokine

The supernatants were collected after the HUVECs were exposed to endosulfan for 24 h. The levels of tumor necrosis factor α (TNF-α), interleukin-1β (IL-1β), and interleukin-6(IL-6) were measured by enzyme-linked immunosorbent assay kits (Yuchen Biotechnology Company, Shanghai) according to the manufacturer's protocols. Briefly, 50 μL of supernatants were added in each well and incubated for 2 h at room temperature. Then, biotin antibody was added to each well and incubated for 1 h. After that, streptavidin solution was added and incubated for 30 min. Next, the substrate reagent was added and incubated for 30 min. After the stop solution was added to each well, the absorbance at 450 nm was detected immediately using a microplate reader (Thermo Multiskan™ MK3; Thermo Fisher Scientific).

2.9. Western blot analysis

Equal amounts of 20 μg of lysate proteins were loaded onto 12% sodium dodecyl sulfate-polyacrylamide gels and electrophoretically transferred to polyvinylidene fluoride (PVDF) membranes (EMD Millipore, Billerica, MA, USA). After blocking with nonfat milk (5%) in Tris-buffered saline (TBS) for 1 h, the PVDF membrane was incubated, respectively, with AMPK-α(Santa Cruz Biothecnology, USA) (1:1000, rabbit antibodies), LC3, *p*-AMPK-α,beclin-1, mTOR, and *p*-mTOR (CST, USA) (1:1000, rabbit antibodies) at 4 °C overnight. Then, the PVDF membrane was rinsed with TBS and Tween 20 (TBST) and incubated with antirabbit immunoglobulin G secondary antibody (CST) for 1 h. After rinsing with TBST for a total of three times, the proteins bound with the antibody were measured by the enhanced chemiluminescence reagent (Thermo Fisher Scientific). Using the Image Lab™ Software (Bio-Rad Laboratories Inc., Hercules, CA, USA), the densitometric analysis of the Western blot results was performed.

2.10. Statistical analysis

The statistical analysis was performed using the SPSS 16.0 software. Five replicate wells were used in each treatment group, and the mean was calculated as the sample size for one independent experiment. The results were analyzed by one-way analysis of variance followed by the least significant difference method for multiple comparisons. Data were expressed as the mean ± standard deviation from three or five independent experiments. If the P value was less than 0.05, differences were considered statistically significant.

3. Results

3.1. Effect of endosulfan on cytokines expression in HUVECs

The expressions of ICAM-1 and MCP- 1 in supernatant were measured by ELISA. As shown in Fig. 1, the production of ICAM-1 and MCP-1 were significantly increased in 6 and 12 μg/ml groups when compared to that of the control. The inhibitor Dor could reduce the levels of proinflammatory factor levels when compared to 12 μg/ml endosulfan treated group ($P < 0.05$).

3.2. Effect of endosulfan on proinflammatory factor expression in HUVECs

The proinflammatory factors were measured as indicators of an inflammatory response after HUVECs were treated with endosulfan for 24 h. As shown in Fig. 2, the secretion of proinflammatory factors (IL-1β,IL-6 and TNF-α) were significantly increased in the 6 and 12 μg/ml groups when compared to that of the control. The inhibitor Dor could reduce the levels of proinflammatory factor levels when compared to 12 μg/ml endosulfan treated group ($P < 0.05$).

3.3. Effect of endosulfan on autophagy in HUVECs

The untreated cells with normally shaped organelles (Fig. 3 b1); HUVECs treated with endosulfan showed multiple cytoplasmic vacuoles (Fig. 3 b2). Some vacuoles containing mitochondria, cytoplasmic materials and electrondense (Fig. 3 b3, b4). The endosulfan-induced autophagy was further verified by assessing the LC3-I/LC3-II conversion. The western blot analysis showed that the LC3-II/LC3-I ratio was significantly elevated in 6, 12 μg/ml groups ($P < 0.05$), suggesting that the autophagic activity was enhanced by endosulfan in a dose-dependent manner (Fig. 7 A). Furthermore, the immunoblot results also demonstrated that the conversion of LC3-I to LC3-II was obviously suppressed by NAC ($P < 0.05$) (Fig. 7A).

The fluorescent dye Monodansylcadaverine (MDC) was used to measure autophagic vacuoles. As shown in Fig. 4A. The HUVECs were stained by MDC in green color, and the fluorescence intensity of MDC-labeled vesicles were increased in a dose-dependent manner in 6,12 μg/ml groups ($P < 0.05$). In addition, the fluorescence intensity of MDC staining in HUVECs cells were relatively sparse and weak after pretreated NAC ($P < 0.05$) but not Dor

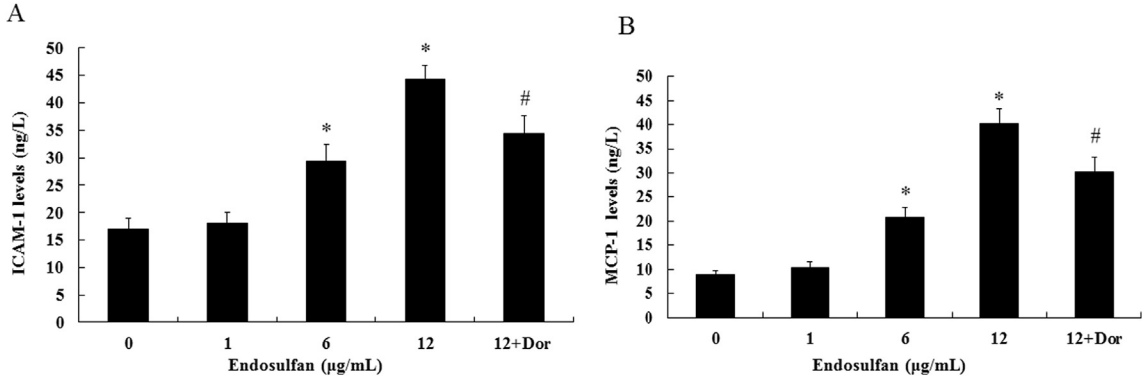

Fig. 1. Effects of endosulfan on the production of cytokines in HUVECs. The expressions of ICAM-1**(A)**and MCP- 1**(B)**were significantly increased in a dose-dependent manner. Data are expressed as the means ± SD from three independent experiments (*$P < 0.05$ versus control group, #$P < 0.05$ versus 12 μg/ml group).

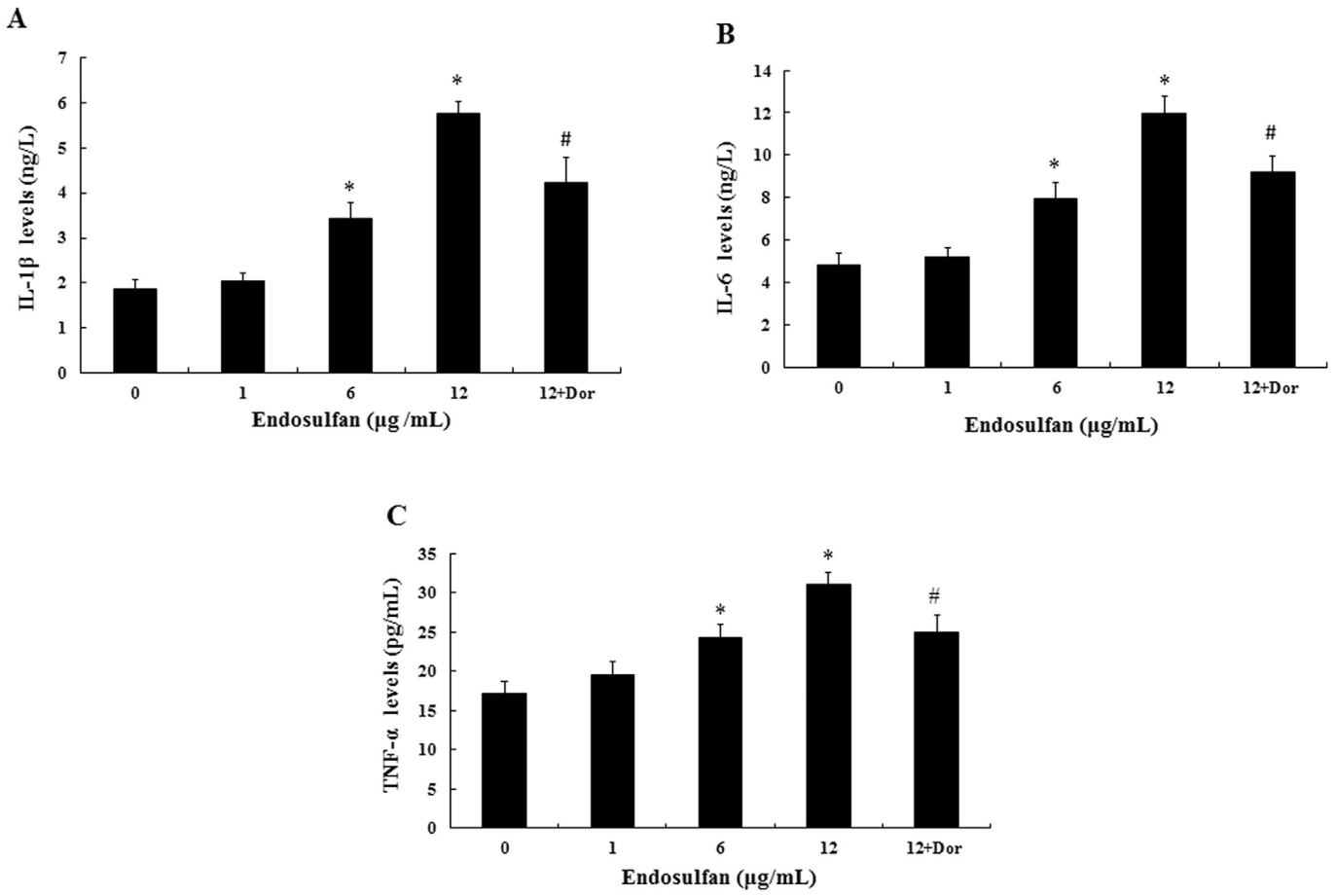

Fig. 2. Effects of endosulfan on proinflammatory factor expression in HUVECs. The production of TNF-α**(A)**, IL-1β**(B)** and IL-6 **(C)** were significantly increased in a dose-dependent manner. Data are expressed as the means ± SD from three independent experiments (*$P < 0.05$ versus control group, #$P < 0.05$ versus 12 μg/ml group).

compared to 12 μg/ml group (Fig. 4B).

3.4. Effect of endosulfan on oxidative stress in HUVECs

The intracellular ROS levels were determined by using the DCFH-DA probe. As shown in Fig. 5A, the ROS levels were elevated gradually in HUVECs with increasing concentrations of endosulfan. The generation of ROS in 6, 12 μg/ml endosulfan treated groups increased significantly compared to control group ($P < 0.05$). Similar to ROS as shown in Fig. 5B, the MDA levels also increased as a dose-dependent manner, and significantly increased in 6, 12 μg/ml endosulfan groups when compared to control group ($P < 0.05$). Moreover, NAC could reduce the levels of ROS and MDA when compared to 12 μg/ml endosulfan treated group ($P < 0.05$).

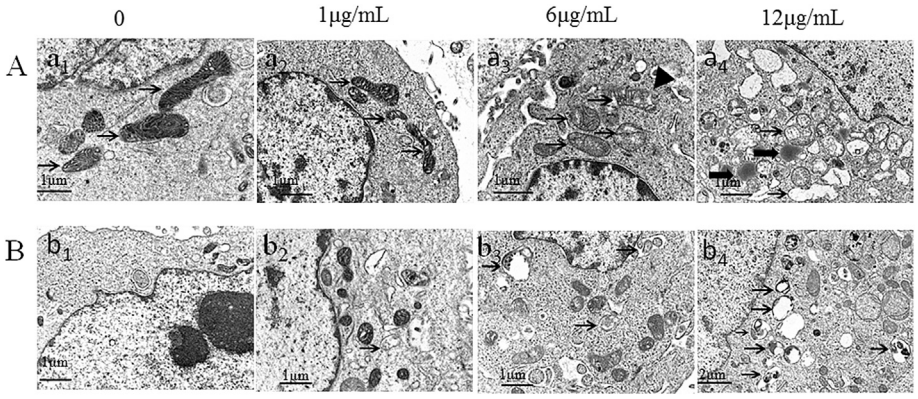

Fig. 3. Autophagy activation and mitochondria injury in HUVECs measured by ultrastructural analysis. (A) The control group displayed the smooth membranes of the mitochondria, and their cristae were arranged regularly and clearly (a1, × 10,000) (black arrows). In contrast, the 1 μg/ml group showed the mitochondrial cristae missed patially (a2, × 10,000) (black arrows), in the 6 μg/ml group, the mitochondria were swollen and more cristae were missing or ruptured (a3, × 10,000) (black arrows). In 12 μg/ml group, the mitochondria were deformed, and vacuolization was observed, the segmental defects were found in the outer and inner membranes of the mitochondria, and almost all of the mitochondrial cristae disappeared (a4, × 10,000) (black arrows). **(B)** Untreated cells with normally shaped organelles (b1 × 10,000); HUVECs treated with endosulfan showing multiple cytoplasmic vacuoles (b2 × 10,000) (black arrows). Some vacuoles containing mitochondria, cytoplasmic materials and electrondense (b3, × 10,000; b4, × 60,000) (black arrows).

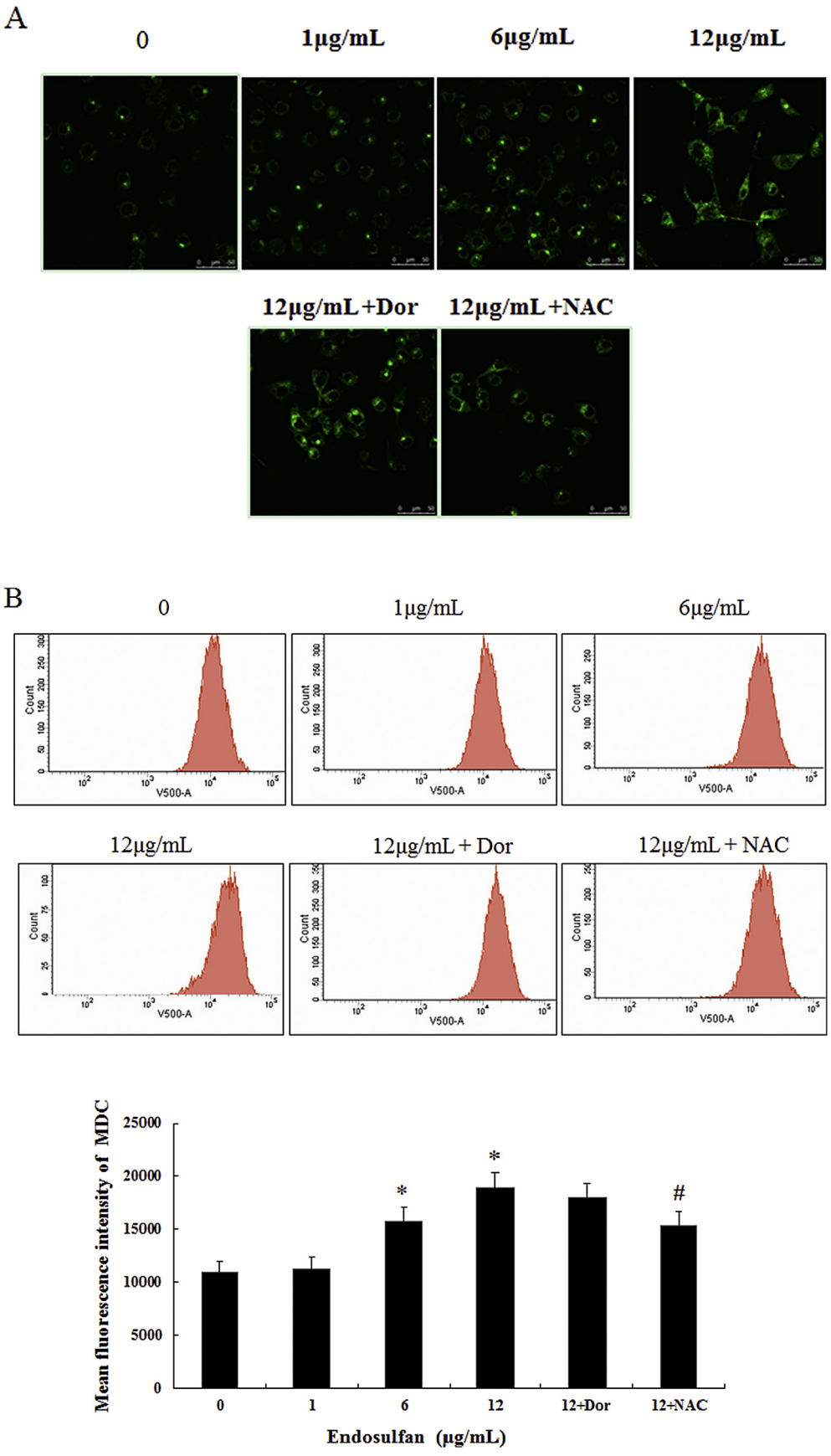

Fig. 4. Detection of autophagic vacuoles induced by endosulfan via MDC staining. (**A**) Confocal microscopy images of MDC staining. (**B**) Quantification of MDC staining by flowcytometry analysis. Data are expressed as means ± SD from five independent experiments (*$P < 0.05$ versus control group, #$P < 0.05$ versus 12 μg/ml group).

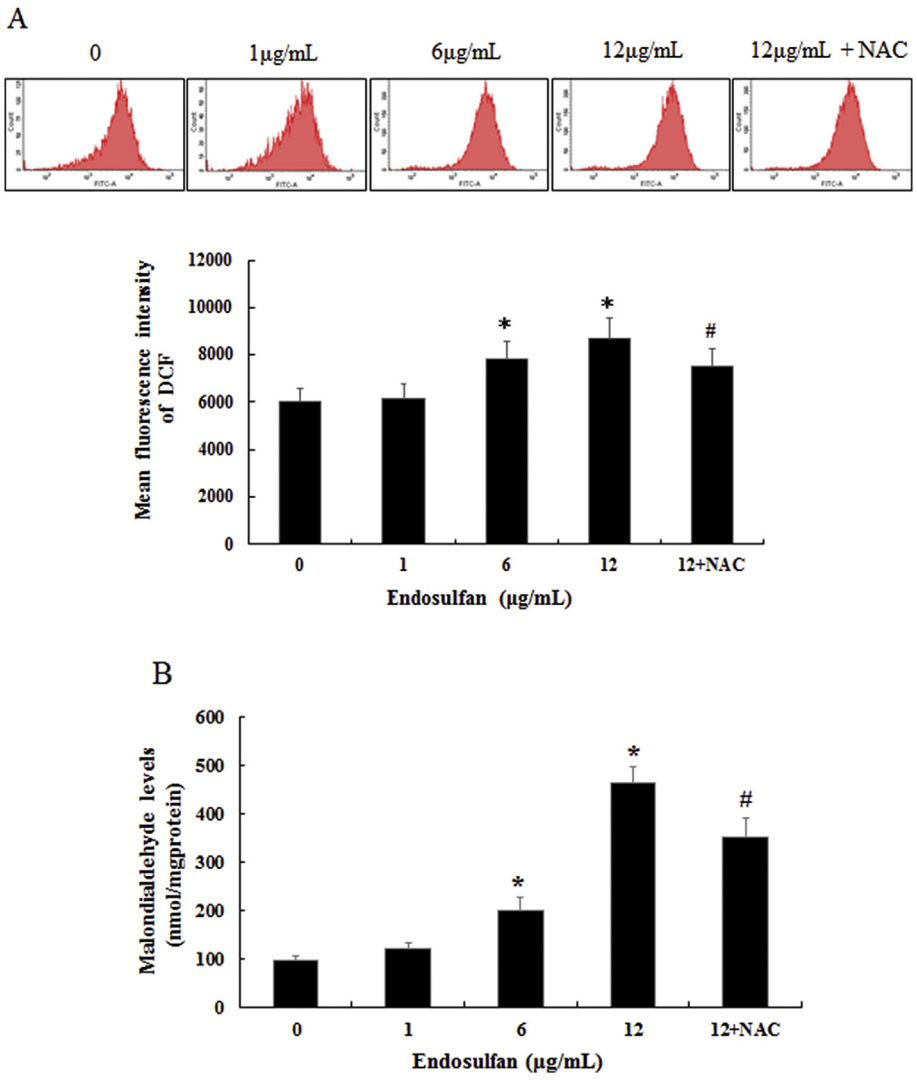

Fig. 5. Effects of endosulfan on ROS and MDA levels. **(A)** The ROS was detected with DCFH probe by flow cytometry. **(B)** The changes of MDA levels. Data are expressed as means ± SD from five independent experiments (*$P < 0.05$ versus control group, #$P < 0.05$ versus 12 μg/ml group).

3.5. Effect of endosulfan on mitochondrial in HUVECs

Mitochondrial membrane potential (MMP), a sign of damage to mitochondrial membrane, was measured by a fluorescent probe 5,5′,6,6'-tetrachloro-1,1′,3,3'- tetraethylbenzimi dazolylcarbocyanide iodine (JC-1). The alteration of MMP was expressed by the ratio of red/green fluorescence intensity. With the dosage increasing, more loss of MMP was caused by endosulfan in 6,12 μg/ml groups compared to control group ($P < 0.05$) (Fig. 6A).

In addition, the damaged mitochondria were observed by ultrastructural analysis. The control group displayed the smooth membranes of the mitochondria, and their cristae were arranged regularly and clearly (Fig. 3). In contrast, the 1 μg/ml group showed the mitochondrial cristae missed partially (Fig. 3 a2), in the 6 μg/ml group, the mitochondria were swollen and more cristae were missing or ruptured (Fig. 3 a3). In 12 μg/ml group, the mitochondria were deformed, and vacuolization was observed, the segmental defects were found in the outer and inner membranes of the mitochondria, and almost all of the mitochondrial cristae disappeared (Fig. 3 a4). After 24 h of endosulfan exposure, the ATP levels in 6,12 μg/ml treatment groups were significantly lower ($P < 0.05$) compared with the control group, However, NAC significantly relieved the decreases of ATP levels caused by endosulfan in 12 μg/ml group ($P < 0.05$) (Fig. 6B).

3.6. Effects of endosulfan on autophagy AMPK-α/mTOR signaling pathway

As shown in Fig. 7, the ratios of *p*-AMPK-αand Beclin-1 in HUVECs were significantly increased, *p*-mTOR decreased in a dose-dependent manner after exposure to endosulfan for 24 h.

4. Discussion

Our previous study showed endosulfan could induce the vascular endothelial cell apoptosis through oxidative stress(Afeseh Ngwa et al., 2011). However, the relationship between endosulfan and autophagy remains unclear. In this study, we explored the relationship between endosulfan-induced autophagic activity and endothelial cell dysfunction, which provided persuasive evidence for the mechanism of atherosclerosis and cardiovascular disease.

The present study indicated that endosulfan induced autophagy and HUVECs dysfunction via oxidative stress and subsequent mitochondria damage. More importantly, results from our present

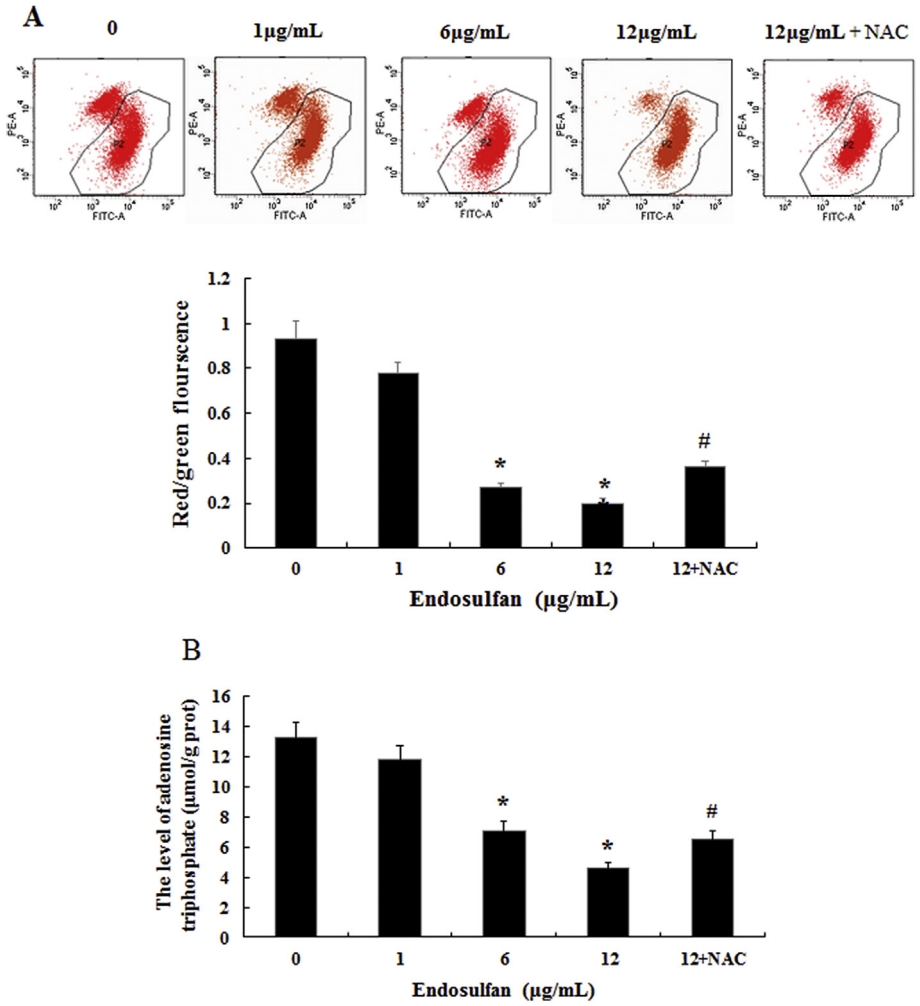

Fig. 6. Effects of endosulfan on mitochondrial membrane potential (MMP) and ATP levels. (A) The MMP was detected with JC-1 probe by flow cytometry. **(B)** The red/green fluorescence intensity ratio was used to express the changes of MMP and the decreased ratio indicates decrease of MMP. **(C)** Total ATP levels were expressed as theμmol/g prot. Data are expressed as means ± SD from five independent experiments ($^{*}P < 0.05$ versus control group, $^{\#}P < 0.05$ versus 12 μg/ml group). (For interpretation of the references to colour in this figure legend, the reader is referred to the web version of this article.)

study also revealed that AMPK phosphorylation, mTOR dephosphorylation played a crucial role of autophagy mediated by endosulfan. These findings consolidated an essential role for endosulfan as an important inducement factors in HUVECs autophagy and related cardiovascular diseases through autophagy regulation.

The results showed the typical autophagic ultrastructures and the damaged mitochondria were found in the TEM images (Fig. 3), and the levels of MMP and ATP in HUVECs also decreased but the ROS and MDA levels increased with the inducing of endosulfan as a dose-dependent manner (Figs. 1 and 2), this was consistent with previous results that endosulfan could induce the damage of mitochondria and ATP decreasing via oxidative stress (Endemann and Schiffrin, 2004; Wu et al., 2011). It was reported that mitochondrial damage had a close connection with autophagy (Green et al., 2011; Dromparis and Michelakis, 2013). The damaged mitochondria can be removed by mitophagy (mitochondria specific autophagy) (Blouin et al., 1977). Given that the vasculature function delivers oxygen rather than consumes it, mitophagy maybe plays a key role in vascular biology. To minimize the oxygen consumption in vasculature, one of the possible mechanisms is to reduce the amount of mitochondria through mitophagy (Green et al., 2011) (Green et al., 2011). In this regard, it is not surprising that the number of mitochondria in endothelial cells is less than that in hepatic cells (Mizushima and Yoshimori, 2007; Klionsky et al., 2012). It indicated that endosulfan induced autophagy in HUVECs via oxidative stress and mitochondria damage.

In order to further confirm the autophagy activation triggered by endosulfan in endothelial cells, MDC staining and LC3-I/LC3-II conversion were employed to detect autophagic vacuoles. Results from MDC staining suggested that endosulfan was the autophagy activator in endothelial cells (Fig. 4). The autophagy protein marker, the protein LC3, from a soluble form (LC3-I) to a lipidized form (LC3-II) when autophagy is activated; thus, the ratio of LC3-II to LC3-I is a standard marker for the detection of autophagy (Dromparis and Michelakis, 2013; Inoue et al., 2010). The present study showed that the ratio of LC3-II/LC3-I had increased significantly in a dose-dependent manner as the beclin-1 buildup (Fig. 7). This was also in line with the results of the MDC expression and the ultrastructural analysis in endothelial cells treated with endosulfan (Figs. 3 and 4). The abnormal induction of autophagy, either from the upregulated or blocked autophagy flux, will result in toxic effects on endothelial cells and on the vascular system. The ability to maintain normal intracellular homeostasis will be reduced if the decrease in mitochondria is below the threshold value in endothelial cells. As a result, this will lead to endothelial cell dysfunction (Shi et al., 2014).

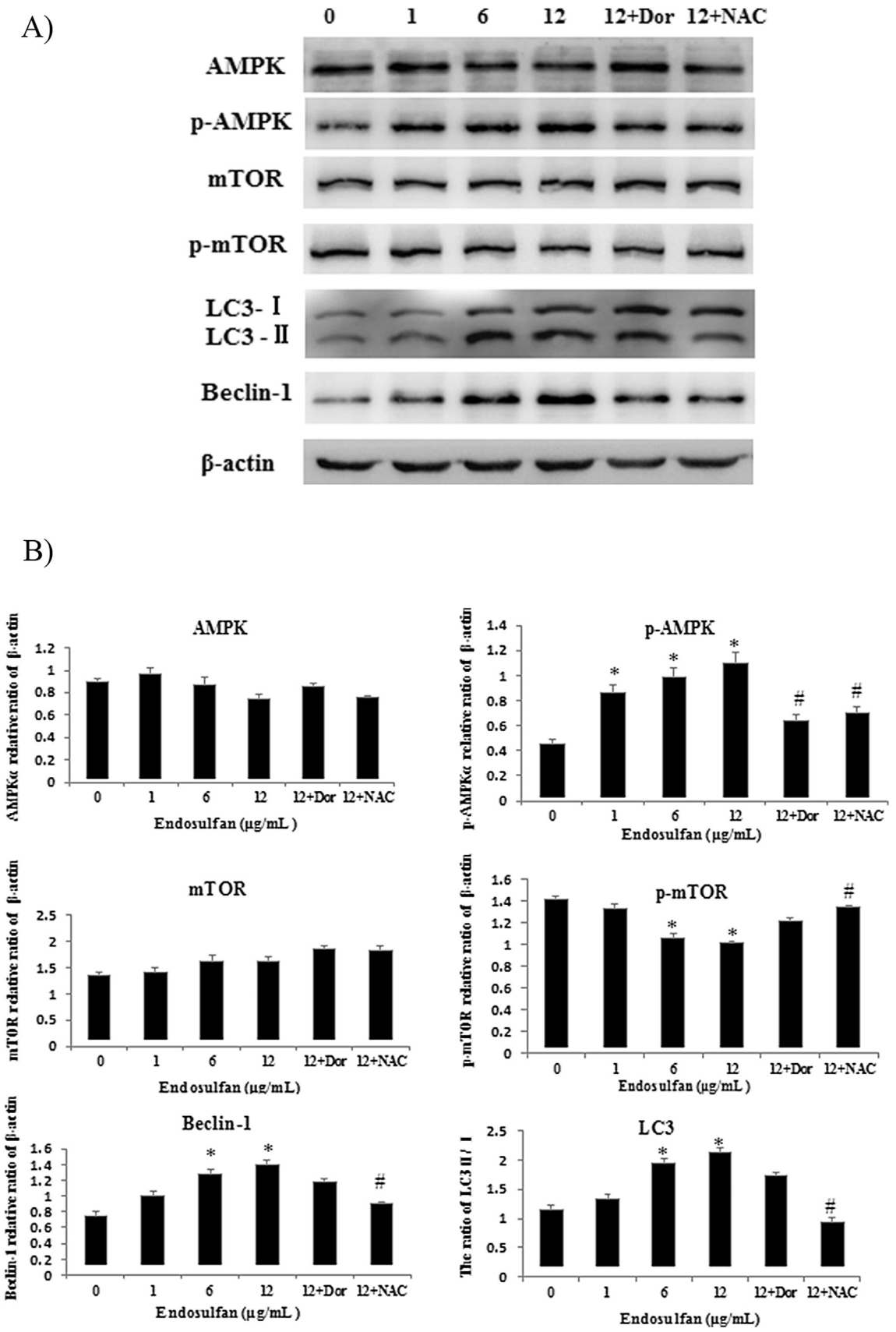

Fig. 7. Effects of endosulfan on autophagy signaling pathways. (A) Effects of endosulfan on the expression of LC3II/I, *p*-AMPK-α, AMPK-α, Beclin-1, *p*-mTOR and mTOR proteins. β-actin was used as an internal control to monitor for equal loading. **(B)** Endosulfan induced autophagy through the up-regulation of AMPK-α/mTOR signaling pathways; Data are expressed as the means ± SD (*$P < 0.05$ versus control group, #$P < 0.05$ versus 12 μg/ml group).

Endothelial cell dysfunction has a potential role in atherosclerosis which partially characterized by chronic inflammation and by an increased expression level of protein biomarkers, such as intercellular adhesion molecule-1 (ICAM-1) and monocyte chemotactic protein-1 (MCP-1) in the activated endothelial cells (Kumar et al., 2014). Given that the MCP-1, ICAM-1 is directly related to endothelial cell functions (Yin et al., 2015), we measured the levels of MCP-1and ICAM-1, in this study, the results showed that endosulfan increased the production of MCP-1, ICAM-1levels with the development of autophagy. Meanwhile, recent studies have identified that PCB was significantly associated with levels of ICAM-1in people blood (Harris, 2011) and there was a link between MCP-1, ICAM-1 and autophagy (Habib, 2011). Moreover, it should be noted that there is crosstalk between autophagy and cytokines in regard to the inflammatory response (Kanamori et al., 2011). The cytokines (TNF-a, IL-1β, and IL-6) have been shown to induce autophagic activity; in contrast, autophagy can regulate the production of proinflammatory cytokines (Kanamori et al., 2011). In the present study, our data demonstrated that endosulfan could enhance the generation of proinflammatory cytokines (TNF-a, IL-1β, and IL-6) (Fig. 7). Similar to our previous findings, exposure to endosulfan could lead to a proinflammatory response in vascular endothelial cells (Endemann and Schiffrin, 2004).

To gain insight into the mechanism of endosulfan-induced autopagic activity and endothelial dysfunction, we examined the AMPK/mTOR signaling pathway by western blot assay (Fig. 7). The serine/threonine kinase mTOR, is inhibited by AMPK, which regulates intracellular energy status by sensing the AMP/ATP ratio. Our results revealed that endosulfan treatment decreased ATP levels, increased the phosphorylation of AMPK and mTOR dephosphorylation, respectively. These findings are consistent with previous findings where rapamycin directly stimulates AMPK and inhibits Mtor (Hahn-Windgassen et al., 2005; Hardie, 2007). Consistent with AMPK phosphorylation and mTOR dephosphorylation, rapamycin promoted autophagy as evidenced by increased LC3II and LC3II-to-LC3I ratio, in agreement with the previous findings (Hahn-Windgassen et al., 2005; Hardie, 2007; Hay and Sonenberg, 2004; Wu and Schwartzman, 2011).

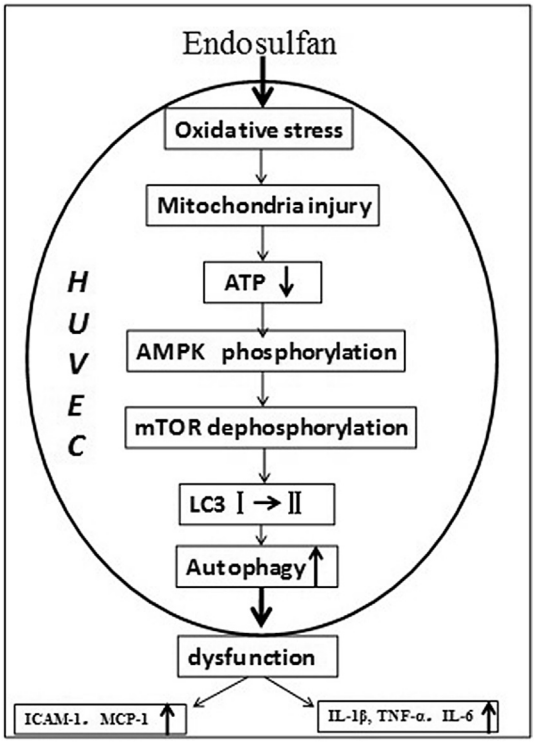

Fig. 8. The schematic diagram of autophagy induced by endosulfan via AMPK/mTOR pathway through oxidative stress. Oxidative stress was induced by endosulfan, and then mitochondria was damaged and AMPK was activated, resulted in autophagy and dysfunction of HUVECs.

In conclusion, our results confirmed that endosulfan induced HUVECs dysfunction, as well as activated autophagy (Fig. 8). The endothelial cell function is of great importance in maintaining vascular homeostasis. Endothelial dysfunction is an initial event that has been implicated in several cardiovascular diseases (Hay and Sonenberg, 2004). Thus, more investigations are required to explore the biological mechanisms of the interaction between autophagy, endothelial dysfunction, and cardiovascular diseases triggered by endosulfan.

Acknowledgments

This research was supported by the National Natural Science Foundation of China (No. 31370430).

References

Afeseh Ngwa, H., Kanthasamy, A., Gu, Y., Fang, N., Anantharam, V., Kanthasamy, A.G., 2011. Manganese nanoparticle activates mitochondrial dependent apoptotic signaling and autophagy in dopaminergic neuronal cells. Toxicol. Appl. Pharmacol. 256, 227–240.
Aggarwal, M., Naraharisetti, S.B., Dandapat, S., Degen, G.H., Malik, J.K., 2008. Perturbations in immune responses induced by concurrent subchronic exposure to arsenic and endosulfan. Toxicology 251, 51–60.
Blouin, A., Bolender, R.P., Weibel, E.R., 1977. Distribution of organelles and membranes between hepatocytes and nonhepatocytes in the rat liver parenchyma. A stereological study. J.Cell. Biol. 72, 441–455.
Catalán, Ú., de Las, López, Hazas, M.C., Rubió, L., Fernández-Castillejo, S., Pedret, A., de la Torre, R., Motilva, M.J., Solà, R., 2015. Protective effect of hydroxytyrosol and its predominant plasmatic human metabolites against endothelial dysfunction in human aortic endothelial cells. Mol. Nutr. Food. Res. 59, 2523–2536.
Choudhary, N., Joshi, S.C., 2003. Reproductive toxicity of endosulfan in male albino rats. Bull. Environ. Contam. Toxicol. 70, 285–289.
Dromparis, P., Michelakis, E.D., 2013. Mitochondria in vascular health and disease. Annu. Rev. Physiol. 75, 95–126.
Endemann, D.H., Schiffrin, E.L., 2004. Endothelial dysfunction. J. Am. Soc. Nephrol. 15, 1983–1992.
Green, D.R., Galluzzi, L., Kroemer, G., 2011. Mitochondria and the autophagy inflammation-cell death axis in organismal aging. Science 333, 1109–1112.
Gregoraszczuk, E.L., Ptak, A., Karniewska, M., Ropstad, E., 2008. Action of defined mixtures of PCBs, p,p'-DDT and its metabolite p,p'-DDE, on co-culture of porcine theca and granulosa cells: steroid secretion, cell proliferation and apoptosis. Reprod. Toxicol. 26, 170–174.
Habib, S.L., 2011. Mechanism of activation of AMPK and upregulation of OGG1 byrapamycin in cancer cells. Oncotarget 2, 958–959.
Hahn-Windgassen, A., Nogueira, V., Chen, C.C., Skeen, J.E., Sonenberg, N., Hay, N., 2005. Akt activates the mammalian target of rapamycin by regulating cellular ATP level and AMPK activity. J. Biol. Chem. 280, 32081–32089.
Hardie, D.G., 2007. AMP-activated/SNF1 protein kinases: conserved guardians of cellular energy. Nat. Rev. Mol. Cell. Biol. 8, 774–785.
Harris, J., 2011. Autophagy and cytokines. Cytokine 56, 140–144.
Hay, N., Sonenberg, N., 2004. Upstream and downstream of mTOR. Genes. Dev. 18, 1926–1945.
Inoue, M., Ishida, T., Yasuda, T., Toh, R., Hara, T., Cangara, H.M., Rikitake, Y., Taira, K., Sun, L., Kundu, R.K., Quertermous, T., Hirata, K., 2010. Endothelial cell-selective adhesion molecule modulates atherosclerosis through plaque angiogenesis and monocyte-endothelial interaction. Microvasc. Res. 80, 179–187.
Jaiswal, A., Parihar, V.K., Sudheer Kumar, M., Manjula, S.D., Krishnanand, B.R., Shanbhag, R., Unnikrishnan, M.K., 2005. 5-Aminosalicylic acid reverses endosulfan-induced testicular toxicity in male rats. Mutat. Res. 585, 50–59.
Jamil, K., Shaik, A.P., Mahboob, M., Krishna, D., 2004. Effect of organophosphorus and organochlorine pesticides (monochrotophos, chlorpyriphos, dimethoate, and endosulfan) on human lymphocytes in-vitro. Drug. Chem. Toxicol. 27, 133–144.
Kanamori, H., Takemura, G., Goto, K., Maruyama, R., Tsujimoto, A., Ogino, A., Takeyama, T., Kawaguchi, T., Watanabe, T., Fujiwara, T., Fujiwara, H., Seishima, M., Minatoguchi, S., 2011. The role of autophagy emerging in post-infarction cardiac remodelling. Cardiovasc. Res. 91, 330–339.
Klionsky, D.J., Abdalla, F.C., Abeliovich, H., Abraham, R.T., Acevedo-Arozena, A., Adeli, K., et al., 2012. Guidelines for the use and interpretation of assays for monitoring autophagy. Autophagy 8, 445–544.
Kumar, J., Lind, P.M., Salihovic, S., van Bavel, B., Ingelsson, E., Lind, L., 2014. Persistent

organic pollutants and inflammatory markers in a cross-sectional study of elderly swedish people: the PIVUS cohort. Environ. Health.Perspect 122, 977–983.
Li, X.Y., Jing, C.Q., Zang, X.Y., Yang, S., Wang, J.J., 2012. Toxic cytological alteration and mitochondrial dysfunction in PC12 cells induced by 1-octyl-3-methylimidazolium chloride. Toxicol. Vitro 26, 1087–1092.
Li, Y., Zhu, H., Wang, S., Qian, X., Fan, J., Wang, Z., Song, P., Zhang, X., Lu, W., Ju, D., 2015. Interplay of oxidative stress and autophagy in PAMAM dendrimers-induced neuronal cell death. Theranostics 5, 1363–1377.
Liu, G.Y., Jiang, X.X., Zhu, X., He, W.Y., Kuang, Y.L., Ren, K., Lin, Y., Gou, X., 2015. ROS activates JNK-mediated autophagy to counteract apoptosis in mouse mesenchymal stem cells in vitro. Acta. Pharmacol. Sin. 36, 1473–1479.
Mersie, W., Seybold, C.A., Mcnamee, C., et al., 2003. A bating endosulfan from runoff using vegetative filter strips: the importance of plant species and flow rate. Agric. Ecosyst. Environ 97, 215–223.
Mizushima, N., Yoshimori, T., 2007. How to interpret LC3 immunoblotting. Autophagy 3, 542–545.
Ozmen, O., Mor, F., 2015. Effects of vitamin C on pathology and caspase-3 activity of kidneys with subacute endosulfan toxicity. Biotech. Histochem 90, 25–30.
Panza, J.A., Quyyumi, A.A., Brush, J.E., Epstein, S.E., 1990. Abnormal endothelium-dependent vascular relaxation in patients with essential hypertension. N. Engl. J. Med. 323, 22–27.
Quan, C., Shi, Y., Wang, C., Wang, C., Yang, K., 2014. p,p'-DDE damages spermatogenesis via phospholipid hydroperoxide glutathione peroxidase depletion and mitochondria apoptosis pathway. Environ. Toxicol. http://dx.doi.org/10.1002/tox.22072.
Shi, J., Sun, X., Lin, Y., Zou, X., Li, Z., Liao, Y., Du, M., Zhang, H., 2014. Endothelial cell injury and dysfunction induced by silver nanoparticles through oxidative stress via IKK/NF-κB pathways. Biomaterials 35, 6657–6666.
Teng, R.J., Du, J., Welak, S., Guan, T., Eis, A., Shi, Y., Konduri, G.G., 2012. Cross talk between NADPH oxidase and autophagy in pulmonary artery endothelial cells with intrauterine persistent pulmonary hypertension. Am. J. Physiol. Lung. Cell. Mol. Physiol. 302, L651–L663.
Wang, X., Liu, Q., Wang, Z., Wang, P., Hao, Q., Li, C., 2009. Bioeffects of low-energy continuous ultrasound on isolated sarcoma 180 cells. Chemotherapy 55, 253–261.
Wu, C.C., Schwartzman, M.L., 2011. The role of 20-HETE in androgen-mediated hypertension. Prosta. Gl. Lipid. Mediat 96, 45–53.
Wu, Y.N., Yang, L.X., Shi, X.Y., Li, I.C., Biazik, J.M., Ratinac, K.R., Chen, D.H., Thordarson, P., Shieh, D.B., Braet, F., 2011. The selective growth inhibition of oral cancer by iron core-gold shell nanoparticles through mitochondria mediated autophagy. Biomaterials 32, 4565–4573.
Yin, J., Wang, Y., Gu, L., Fan, N., Ma, Y., Peng, Y., 2015. Palmitate induces endoplasmic reticulum stress and autophagy in mature adipocytes: implications for apoptosis and inflammation. Int. J. Mol. Med. 35, 932–940.
Zhang, L., Wei, J., Guo, F., Duan, J., Li, Y., Shi, Z., Yang, Y., Zhou, X., Sun, Z., 2015. Endosulfan activates the extrinsic coagulation pathway by inducing endothelial cell injury in rats. Environ. Sci. Pollut. Res. 22, 15722–15730.